SLAC – PUB – 3437
September 1984
T/E

HEAVY FAMILIES: MASSES AND MIXINGS*

JONATHAN BAGGER

Stanford Linear Accelerator Center
Stanford University, Stanford, California, 94305

SAVAS DIMOPOULOS†
Department of Physics
Stanford University, Stanford, California, 94305

EDUARD MASSÓ‡

Stanford Linear Accelerator Center
Stanford University, Stanford, California, 94305

Submitted to *Nuclear Physics B*

---

* Work supported by the Department of Energy, contract DE-AC03-76SF00515, and by the National Science Foundation, contract NSF-PHY-83-10654.

† Alfred P. Sloan Foundation Fellow.

‡ Fulbright Fellow. On leave of absence from Departament de Física Teòrica, Universitat Autónoma de Barcelona, Bellaterra, Spain.

ABSTRACT

We use the infrared fixed point structure of the SU(3) $\times$ SU(2) $\times$ U(1) renormalization group equations to derive predictions for the masses and mixings of heavy families in perturbatively unifiable grand unified theories. We show that the sum of the squares of all quark (or lepton) masses must be less than $(355\ \text{GeV})^2$. This implies that theories with N_H heavy families must have at least one new quark and one new lepton of mass less than $250/\sqrt{N_H}$ GeV. We also find that the Cabibbo mixings and isospin splittings of heavy quarks tend to be small.

1. Introduction

The coming generation of particle accelerators will start to probe the physics beyond the standard SU(3) $\times$ SU(2) $\times$ U(1) model of the strong, weak and electromagnetic interactions. While it is certainly possible that nothing new will be found, a variety of theoretical arguments suggest that new quarks and leptons should appear below the TeV scale.

In this paper we derive strong constraints on the masses and mixings of extra standard-model families in grand unified theories. Our results follow from a renormalization group analysis of the usual SU(3) $\times$ SU(2) $\times$ U(1) gauge and Yukawa couplings. We make only two assumptions. The first is that of a desert. We assume that SU(3) $\times$ SU(2) $\times$ U(1) is the effective gauge theory between the weak scale M_W and the grand unification scale M_X. The second is that of perturbative unification. We require all gauge and Yukawa couplings to be small enough for perturbation theory to be valid all the way up to the scale M_X. This second assumption is an essential requirement for grand unification. Subject to these restrictions, we place rigorous upper bounds on the sums of the squares of the quark masses,

$$\sum_Q {M_Q}^2 \lesssim (355 \text{ GeV})^2 , \tag{1.1}$$

and of the lepton masses,

$$\sum_L {M_L}^2 \lesssim (330 \text{ GeV})^2 . \tag{1.2}$$

The inequalities (1.1) and (1.2) lead immediately to stringent upper bounds on the masses of individual quarks and leptons. In theories with extra heavy families, equations (1.1) and (1.2) imply that the lightest new quarks or leptons must obey the following relations,

$$\begin{aligned} m_Q &\lesssim (250/\sqrt{N_H}) \text{ GeV} \\ m_L &\lesssim (235/\sqrt{N_H}) \text{ GeV} , \end{aligned} \tag{1.3}$$

where N_H denotes the number of new heavy families.

The above bounds should be compared with the naive bound of $M_Q = g_Q \langle \phi \rangle \lesssim 2$ TeV, which follows from insisting that perturbation theory be valid at the weak scale. The 2 TeV limit holds for each quark and lepton individually, so the sum over all quarks and leptons is even less restrictive. Other limits on fermion masses follow from partial-wave unitarity [1], from the fact that the ρ parameter is so close to one [2], and from SU(2) $\times$ U(1) vacuum stability [3]. Partial-wave unitarity gives the restrictions $M_Q \lesssim 500/\sqrt{N_D}$ GeV and $M_L \lesssim 1000/\sqrt{N_D}$ GeV, where N_D denotes the number of nearly degenerate standard-model families. Measurements of the ρ parameter limit isodoublet mass splittings to be less than 500 GeV, but they do not restrict individual fermion masses. Finally, SU(2) $\times$ U(1) vacuum stability implies the bound $\sum {M_Q}^4 \lesssim (900 \text{ GeV})^4$. In comparison to these bounds, we see that the renormalization group constraints (1.1) through (1.3) are really quite restrictive. They imply that extra standard-model families—if they exist at all—should soon be found.

Our renormalization group analysis implies much more than the bounds discussed above. It also demonstrates the following features of the heavy quark and lepton mass spectra:

- The bounds (1.1) and (1.2) are rigorous for grand unified theories with any number of perturbatively unifiable families. If there are fewer than eight such families, the bounds can be tightened still further. For most initial conditions, the lepton bound (1.2) is far from being saturated. As a consequence, lepton masses tend to be much smaller than quark masses.

- The Cabibbo mixings of heavy families with each other and with light families tend to be small. This implies that some heavy quarks in a wide range of models should have relatively long lifetimes.

- Each heavy up-type quark tends to form a weak doublet with the down-type quark closest in mass. That is to say, isospin breaking tends to vanish in the heavy quark limit.

These results follow from an extensive analysis of the renormalization group equations for Yukawa couplings in grand unified theories. They rely on the fact that these equations have a rich infrared fixed point structure [4,5,6]. In the next section we give a general analysis of this fixed point structure. We distinguish mathematical from physical fixed points, and discuss the implications of each. In Section 3 we discuss what we call the radial fixed point. We demonstrate that the radial fixed point leads to the bounds mentioned above. In Section 4 we define the angular fixed point. We show that the angular fixed point controls the evolution of the Cabibbo angles and the isospin breaking. In Section 5 we illustrate the role of initial conditions in determining the low energy spectrum of a grand unified theory. In Section 6 we examine the evolution of light quarks and leptons in the presence of heavy families. We show that light quark and lepton mass ratios renormalize by constant, calculable amounts that depend only on the number of heavy families, and not on their masses. We conclude with a summary of our most important results in Section 7.

2. Infrared Fixed Points of the Renormalization Group Equations

In this section we begin our discussion of the renormalization group equations for Yukawa couplings in grand unified theories. We consider grand unified theories in which a simple group G breaks to SU(3) $\times$ SU(2) $\times$ U(1) at a mass scale M_X of order 10^{15} GeV. We assume that the spectrum of the theory below M_X contains N_F standard-model families, along with one Higgs doublet and the usual SU(3) $\times$ SU(2) $\times$ U(1) gauge bosons. We denote the $N_F \times N_F$ Yukawa coupling matrices Y by U, D, E, and N, for up quarks, down quarks, charged leptons, and neutrinos, respectively.*

In this notation, the one-loop renormalization group equations for the Yukawa

* We assume, for generality, that the low energy theory contains right-handed neutrinos. If there are no such neutrinos, then $N = 0$.

couplings take the following form [7],

$$Y^{-1}\frac{dY}{dt} = G_Y - T - \frac{3}{2}S_Y \ , \tag{2.1}$$

where

$$\begin{aligned}
S_U &= U^\dagger U - D^\dagger D \ , \qquad G_U = 8\,{g_3}^2 + \frac{9}{4}{g_2}^2 + \frac{17}{20}{g_1}^2 \ ; \\
S_D &= D^\dagger D - U^\dagger U \ , \qquad G_D = 8\,{g_3}^2 + \frac{9}{4}{g_2}^2 + \frac{1}{4}{g_1}^2 \ ; \\
S_E &= E^\dagger E - N^\dagger N \ , \qquad G_E = \frac{9}{4}{g_2}^2 + \frac{9}{4}{g_1}^2 \ ; \\
S_N &= N^\dagger N - E^\dagger E \ , \qquad G_N = \frac{9}{4}{g_2}^2 + \frac{9}{20}{g_1}^2 \ ; \\
T &= \mathrm{Tr}\left[3U^\dagger U + 3D^\dagger D + E^\dagger E + N^\dagger N\right] \ .
\end{aligned} \tag{2.2}$$

Here g_3, g_2, and g_1 are the SU(3) $\times$ SU(2) $\times$ U(1) gauge couplings, and[†]

$$t = -\frac{1}{16\pi^2}\log\left(\frac{M}{M_X}\right) \ . \tag{2.3}$$

It is important to note that the gauge contributions to (2.1) tend to increase the fermion masses at low energies, while the Yukawa contributions tend to make them smaller. It is this competition between the gauge and Yukawa terms that leads to a fixed point behavior in the low energy theory.

To understand this fixed point structure, we shall neglect the hypercharge coupling g_1. For the moment, we shall also neglect the evolution of g_2 and g_3. In this case, we have $G_U = G_D = \overline{G}_Q$ and $G_E = G_N = \overline{G}_L$, where $\overline{G}_Q$ and $\overline{G}_L$ are constants. When $\overline{G}_Q$ and $\overline{G}_L$ are constant, it is easy to show that the equations (2.1) have two distinct fixed points:

† We have defined t such that an increase in t corresponds to a decrease in the energy M.

1) The quark fixed point, with

$$T = \overline{G}_Q \qquad \text{(radial quark fixed point)} \tag{2.4}$$

$$U^\dagger U = D^\dagger D \qquad \text{(angular quark fixed point)} \tag{2.5}$$

$$E = N = 0\,; \tag{2.6}$$

2) The lepton fixed point, with

$$T = \overline{G}_L \qquad \text{(radial lepton fixed point)} \tag{2.7}$$

$$E^\dagger E = N^\dagger N \qquad \text{(angular lepton fixed point)} \tag{2.8}$$

$$U = D = 0\,. \tag{2.9}$$

Equations (2.4) and (2.7) are incompatible, so the two fixed points cannot be realized simultaneously. Only one of the fixed points is reached in the mathematical limit $t \to \infty$. If the quark fixed point is reached, equation (2.4) determines the overall scale of the quark masses. In this case equation (2.5) implies that all left-handed Cabibbo angles and CP-violating phases vanish. It also implies that each up-type quark has a degenerate down-type partner.

Precisely which of the two fixed points is reached depends on their relative stability and on the initial values of the gauge and Yukawa couplings at $t = t_X = 0$. For physical gauge couplings, we shall see that the quark fixed point is strongly preferred. It has a much larger domain of attraction than the lepton fixed point.

It is important to note that the fixed point conditions (2.4) – (2.9) do not completely determine the spectrum of the low energy theory. Some physical parameters are determined by the initial conditions. At the quark fixed point, the physical masses, mixing angles and CP-violating phases are completely determined by the matrices $U^\dagger U$ and $D^\dagger D$. These $N_F \times N_F$ hermitian matrices

contain ${N_F}^2 + 1$ physical parameters. However, equations (2.4) and (2.5) give ${N_F}^2 - N_F + 2$ relations between the parameters. The remaining $N_F - 1$ relations are not determined by the fixed point conditions. They correspond to conserved quantities that must be specified as initial conditions at the grand unification scale M_X.

There are three important differences between the *mathematical* fixed points defined by equations (2.4) – (2.9) and the *physical* fixed points of a realistic grand unified theory. In a realistic theory, g_1 does *not* vanish, the gauge couplings are *not* constant, and the physical range of t is *finite*—not infinite.

How do these changes affect our previous conclusions? Let us address each in turn:

1) The fact that g_1 does not vanish is unimportant because g_1 is much smaller than g_2 or g_3.

2) The evolution of the gauge couplings with t can be taken into account [5] by replacing G_Q and G_L with appropriate averages $\overline{G}_Q$ and $\overline{G}_L$. This can be done because the physical range of t is rather short, spanning the interval between $t_X = 0$ and $t_W = -(1/16\pi^2)\log(M_W/M_X) \sim 1/5$. In this range, the gauge couplings are essentially constant.

3) The finite range of t suggests that the Yukawa couplings might not reach fixed points in the limited "time" available [5]. Physical fixed points can only be reached if the Yukawa couplings are sufficiently large. The critical magnitude depends on the fixed point under consideration, and must be found by numerical analysis. As we will see in the next few sections, the radial quark fixed point tends to be reached for a wide range of initial conditions. The angular fixed point, however, is only reached if the initial Yukawa couplings are large.

3. The Radial Fixed Point

In this section we shall begin to discuss the physical fixed points that arise in realistic grand unified theories. We will start with an analysis of the radial fixed point. To that end, we define

$$\begin{aligned} T_Y &= \mathrm{Tr}\, Y^\dagger Y \\ T_Q &= T_U + T_D \\ T_L &= T_E + T_N \\ T &= 3\,T_Q + T_L\,, \end{aligned} \tag{3.1}$$

where $Y = U,\ D,\ E$ or N. Neglecting g_1, we take $G_U = G_D = G_Q$, $G_E = G_N = G_L$, where G_Q and G_L depend on t, and run according to the standard evolution equations for the gauge couplings. In this limit, the evolution of T_Q and T_L is given by [6]

$$\frac{dT_Q}{dt} = 2\,(G_Q - T)\,T_Q - 3\mathrm{Tr}\,(S_U{}^2) \tag{3.2}$$

$$\frac{dT_L}{dt} = 2\,(G_L - T)\,T_L - 3\mathrm{Tr}\,(S_E{}^2)\,. \tag{3.3}$$

Equations (3.2) and (3.3) show that the evolution of T_Q and T_L depend not only on T_Q and T_L themselves, but also on the matrices S_Y. To simplify the analysis still further, we drop the terms that depend on S_Y. (They will be included later in this section.) With $S_Y = 0$, equations (3.2) and (3.3) take the following form,

$$\frac{dT_Q}{dt} = 2\,(G_Q - T)\,T_Q \tag{3.4}$$

$$\frac{dT_L}{dt} = 2\,(G_L - T)\,T_L\,. \tag{3.5}$$

The new equations involve only the traces T_Q and T_L. They do not depend on the matrix structure of U, D, E or N. The equations (3.4) and (3.5) can be solved numerically. Their solution depends implicitly on the total number of families through the gauge couplings G_Q and G_L.

In Figure 1 we have plotted the solution of (3.4) and (3.5) in the eight family case. We follow the evolution of T_Q and T_L from t_X to t_W for a variety of initial conditions, and we see that equations (3.4) and (3.5) possess a rich fixed point structure. There is a radial quark fixed point, corresponding to $\overline{G}_Q = 12.3$ in equation (3.4). There is also a radial lepton fixed point, corresponding to $\overline{G}_L = 10.8$ in (3.5).

As is evident from Figure 1, an overwhelming majority of initial conditions evolve to the quark fixed point. Most initial conditions reach the radial fixed point $\overline{G}_Q = 3T_Q$ in the physical time $0 < t < 1/5$. In contrast, the lepton fixed point is approached for only a small range of initial conditions. The lepton fixed point is approached only for initial conditions that correspond to very large lepton masses and very small quark masses.

It is easy to show that the quark fixed point of equations (3.4) and (3.5) is stable, whereas the lepton fixed point is not. This is clear in Figure 1; several trajectories are initially drawn towards the lepton fixed point, but as time goes on, they are pushed gradually away. The fact that the radial quark fixed point is reached in physical times for most initial conditions has important phenomenological consequences. It implies that new heavy quarks should be significantly heavier than their leptonic partners.

Why is the radial quark fixed point reached in such a short time? The answer lies in equations (3.4) and (3.5). For constant gauge couplings $\overline{G}_Y$, these equations can easily be solved. In the limit $T_L = 0$, one finds

$$\frac{\overline{G}_Q}{3T_Q(t)} = \left\{1 - \left[1 - \frac{\overline{G}_Q}{3T_Q(t_X)}\right] \exp(-2\overline{G}_Q t)\right\} . \qquad (3.6)$$

The fixed point corresponds to $\overline{G}_Q = T = 3T_Q$. With eight families, $\overline{G}_Q = 12.3$,

and similarly, with four families, $\overline{G}_Q = 8.1$. In either case the exponential is strongly damped. Unless $T_Q(t_X)$ is very small, the second term is negligible even at $t = t_W = 1/5$. When this is the case, the fixed point is reached in physical time.

As we have seen, equations (3.4) and (3.5) exhibit fixed point behavior. If the initial traces are large, the fixed point $\overline{G}_Q = 3T_Q$ is reached in physical time. If the initial traces are small, the fixed point is not reached in the available time. This is shown in Figure 2(a), where we have set $S_Y = T_L = 0$, and have graphed T_Q at the weak scale as a function of T_Q at the grand unification scale. It is immediately apparent that the fixed point behavior of T_Q can be summarized in the form of a bound, $\overline{G}_Q \gtrsim 3T_Q$, where $\overline{G}_Q$ is evaluated at the the quark fixed point (indicated by the dotted line in Figure 2(a)). Including the terms T_L and S_Y does not violate this bound, because they enter equations (3.2) and (3.3) with a negative sign. The quark fixed point gives a rigorous upper bound on the value of T_Q at the scale t_W.

A similar analysis can be made for the lepton fixed point T_L (see Figure 2(b)). It leads to a rigorous upper bound on T_L. In the eight family case, the bounds on T_Q and T_L are given by

$$\left.\begin{array}{l} T_Q \lesssim 4.1 \\ T_L \lesssim 3.6 \end{array}\right\} \quad \text{for eight families.} \tag{3.7}$$

In the four family case, we find

$$\left.\begin{array}{l} T_Q \lesssim 2.7 \\ T_L \lesssim 3.4 \end{array}\right\} \quad \text{for four families.} \tag{3.8}$$

These bounds hold at the weak scale t_W. They are equivalent to the following mass inequalities:

$$\left.\begin{aligned} \sum {M_Q}^2 &\lesssim (355\ \text{GeV})^2 \\ \sum {M_L}^2 &\lesssim (330\ \text{GeV})^2 \end{aligned}\right\} \quad \text{for eight families,} \tag{3.9}$$

and

$$\left.\begin{aligned} \sum {M_Q}^2 &\lesssim (290\ \text{GeV})^2 \\ \sum {M_L}^2 &\lesssim (325\ \text{GeV})^2 \end{aligned}\right\} \quad \text{for four families,} \tag{3.10}$$

where all masses are evaluated at the weak scale M_W. For five, six or seven families, the results interpolate between those given above. Theories with more than eight families are not perturbatively unifiable (see Figure 3). Thus the eight-family bounds are strict upper bounds for the quark and lepton masses at the weak scale M_W. They are rigorous upper bounds that are independent of the total number of families. They allow us to conclude that if no new quarks and leptons are found below 355 GeV, the possibility of new (perturbatively unifiable) standard-model families is automatically excluded.

The bounds (3.7) and (3.8) imply more than the inequalities (3.9) and (3.10). They also give an upper bound on the mass of the lightest heavy family. If a theory has N_H heavy families, this bound is found by replacing the sums over ${M_Q}^2$ and ${M_L}^2$ by $2\,N_H$ times m_Q and m_L, where m_Q and m_L denote the masses of the lightest heavy quarks and leptons. This gives

$$\begin{aligned} m_Q &\lesssim (250/\sqrt{N_H})\ \text{GeV} \\ m_L &\lesssim (235/\sqrt{N_H})\ \text{GeV}\ . \end{aligned} \tag{3.11}$$

Equation (3.11) implies that if there are any extra standard-model families, at least one new quark and one new lepton must be found below 250 GeV.* Furthermore, perturbatively unifiable eight-family models must contain at least one new quark and one new lepton below 110 GeV!

* Except, of course, for the top quark.

To further illustrate the radial fixed point, and to improve the bounds in special cases, we now turn to two examples. In these examples we use the complete renormalization group equations (2.1). These equations include the terms $\mathrm{Tr}\,(S_U{}^2)$ and $\mathrm{Tr}\,(S_E{}^2)$ that we dropped in deriving equations (3.4) and (3.5). We shall see that for Yukawa couplings of order 0.5 (or greater), the extra trace terms make very little difference. For large Yukawa couplings, the bounds (3.7) and (3.8) on T_Q tend to be saturated by the sum over all heavy quarks.

For our first example, we consider the four-family case. We assume, however, that three of the families are light, so the one heavy family dominates the mass matrices and traces. We also assume that the fourth heavy family has negligible Cabibbo mixing with its three light partners.

To follow the evolution of the Yukawas, we first set $E = N = 0$. This is entirely consistent with our previous observation that the quark fixed point is reached for most initial conditions. We denote the Yukawa couplings of the heavy up- and down-type quarks by u and d. The evolution of u and d is plotted in Figure 4 for a variety of initial conditions. Each line carries an arrow indicating the flow of t, from t_X to t_W.

The first thing we note is the presence of the radial fixed point, indicated by the dotted circle in Figure 4 [5]. The dotted circle corresponds to $T_Q = 2.7$, as given in equation (3.8). When both Yukawa couplings are large, on the order of 0.5 or greater, the bound (3.8) is saturated in physical times. When both Yukawas are small, T_Q never reaches the bound. And when one Yukawa is large and the other is small, the bound (3.8) is almost achieved—but not quite. This is no surprise, for when either u or d is small, equation (3.2) gives an even tighter bound on T_Q:

$$T_Q \equiv u^2 \lesssim 1.6 \qquad (d = 0)\,. \tag{3.12}$$

This tighter bound is saturated for trajectory (α) in Figure 4. Equation (3.12) restricts the mass of a single extra heavy quark to be less than 220 GeV [8].

In Figure 5 we graph the evolution of T_Q with energy for the initial conditions of Figure 4. We see that the fixed point is approached very rapidly. For most initial conditions, the radial fixed point is reached by 10^{12} GeV, in about 0.04 units of time. Note that below 10^5 GeV, the value of T_Q at the fixed point gradually rises. This reflects the fact that the average coupling $\overline{G}_Q$ gradually changes with t. The rise of T_Q can be understood with the help of Figure 6, where we have sketched T and G_Q versus energy. Above 10^5 GeV, we see that $T > G_Q$. In this regime, equation (3.4) implies that T_Q must decrease. At about 10^5 GeV, the two curves cross. Below that scale, $T < G_Q$, and the value of T_Q slowly increases.

Finally, we discuss the leptons of the heavy fourth family. For simplicity, we assume that the neutral lepton is massless. In this case, equation (3.3) reduces to the following form,

$$\frac{de}{dt} = e\left[G_E - 3u^2 - 3d^2 - \frac{5}{2}e^2\right] . \tag{3.13}$$

where e denotes the Yukawa coupling of the fourth charged lepton. From our previous discussion we know that $u^2 + d^2$ runs rapidly to the quark fixed point T_Q. Since $3T_Q \gg G_E$, it is clear that equation (3.13) has no fixed point. This is evident in Figure 7, where we have graphed the evolution of e for a variety of initial conditions (with $3T_Q = \overline{G}_Q$ at the scale M_X). Note that below 10^{13} GeV, e runs with a constant logarithmic velocity, as expected from equation (3.13).

For our second example, we consider two heavy families and three light families. As before, we use the full renormalization group equations (2.1). Since the effects of weak mixing will be treated in the next section, we set all mixing angles to zero. Family conservation ensures that this condition is stable under radiative corrections.

We define u_1, d_1 and u_2, d_2 to be the Yukawa couplings of the first and second heavy families, respectively. For the sake of presentation, we set $u_1 = d_1$ and $u_2 = d_2$ as initial conditions, and plot the evolution of $\sqrt{u_1 d_1}$ versus

$\sqrt{u_2 d_2}$. Because of isospin symmetry, the conditions $u_1 = d_1$ and $u_2 = d_2$ are also preserved by renormalization (up to small hypercharge effects).

The plot of $\sqrt{u_1 d_1}$ versus $\sqrt{u_2 d_2}$ is shown in Figure 8. The radial fixed point is indicated by the dotted circle of radius squared $T_Q \equiv \sum({u_i}^2 + {d_i}^2) = 2.9$. As expected, the fixed point is reached in physical times. Note, however, that the Yukawa couplings appear to converge to a smaller circle than that indicated by the dots. This is an illusion. What really happens is that the Yukawa couplings quickly run to the minimum radius, and then turn around and run back to the dots at time t_W. As in the previous example, the Yukawas turn around because $\overline{G}_Q$ gradually increases with time. To see how quickly the radial fixed point is reached, we plot $T_Q \equiv \sum({u_i}^2 + {d_i}^2)$ versus energy in Figure 9. As in Figure 5, we see that the radial fixed point is reached very quickly.

With two heavy families, there is only one renormalization group invariant. In the absence of Cabibbo mixing, it is given by

$$\frac{d}{dt} \log\left(\frac{u_1 d_1}{u_2 d_2}\right) = 0 . \tag{3.14}$$

This constant of the motion preserves the polar angle in Figure 8. At the scale t_W, the overall magnitudes of the Yukawa couplings are determined by the radial fixed point T_Q. The ratio $u_1 d_1 / u_2 d_2$, however, is determined by the initial conditions.

4. The Angular Fixed Point

In this section we discuss the angular quark fixed point,*

$$U^\dagger U = D^\dagger D . \tag{4.1}$$

As expected, the angular fixed point (4.1) does not restrict the *unphysical* right-handed Kobayashi-Maskawa matrix. This is because right-handed rotations do

* We do not analyze the lepton fixed point since it is unstable.

not affect the fixed point condition. In contrast, equation (4.1) severely restricts the *physical* left-handed mixing matrix [6]. It implies that the same left-handed unitary matrices diagonalize $U^\dagger U$ and $D^\dagger D$. In an appropriate basis, this simply says that the left-handed Kobayashi-Maskawa matrix $V_L \equiv L_U^\dagger L_D = 1$.

It is important to note that equation (4.1) implies more than the vanishing of the mixing angles. It also implies that each up-type quark has a down-type partner degenerate in mass. The mass doublets, however, do not necessarily correspond to the weak doublets. Barring degeneracies, equation (4.1) contains $N_F!$ fixed points, one for each possible pairing of the quark masses. Only one pairing identifies the mass doublets with the weak doublets. We shall see that this is the only stable fixed point. The SU(3) $\times$ SU(2) $\times$ U(1) renormalization group equations prefer properly paired weak doublets.

The standard SU(3) $\times$ SU(2) $\times$ U(1) Lagrangian does not conserve either isospin or family number. The stable fixed point, however, preserves both $SU(2)_V$ isospin and $U(1)^{N_F}$ family symmetry. The fixed point has greater symmetry than the Lagrangian itself. The SU(3) $\times$ SU(2) $\times$ U(1) renormalization group equations provide a new and important example of an infrared restoration of a global symmetry [9].

The angular fixed point implies that all flavor mixings and isospin splittings vanish in the limit $t \to \infty$. However, in a realistic grand unified theory, the story is more complicated. There might not be enough time for the mathematical fixed point to be reached. To investigate this question, we turn to numerical analysis and examine the evolution of the Cabibbo angles and isospin breaking. These are logically independent quantities, and there is no reason to assume that they run at the same rates. In fact, we shall see that the Cabibbo mixings run somewhat faster than the isospin splittings.

In the remainder of this section, we examine the angular fixed point for the cases of one and two heavy families. These are the same examples that we used previously to illustrate the radial fixed point. We shall see that the angular fixed

point is approached more slowly that the radial fixed point of Section 3.

To begin, we consider one heavy family and three light families. As before, we assume that the one heavy family has no Cabibbo mixings with the three light families. In this case the angular condition (4.1) implies that the heavy Yukawas u and d must be equal. The rate of approach to the angular fixed point is given by

$$\frac{d}{dt} \log \left(\frac{u}{d}\right) = -3(u^2 - d^2) + \frac{3}{5} {g_1}^2 , \tag{4.2}$$

where g_1 is the hypercharge coupling. The evolution of u versus d is shown in Figure 4. This figure was introduced previously to illustrate the radial fixed point. Note that all large Yukawas reach the radial fixed point, but very few of them also achieve the angular fixed point, given by $u = d$ in Figure 4. This can be understood by comparing equations (3.2) and (4.2), and noticing that in general $|u^2 - d^2| \ll |G_Q - T|$. The approach to the angular fixed point is shown in Figure 10, where we plot u/d versus $u^2 + d^2$ for a variety of initial conditions (with $d = 1$ at $t = 0$). Isospin violations of order 1000% decrease to about 50% by the time t_W. The evolutions of T_Q and u/d with energy are compared in Figure 11.

We now turn to the case of two heavy families and three light families. As before, we assume there are no mixings between the heavy and light families. In this case, the angular fixed point reduces to three conditions. One sets the Cabibbo angle to zero, and the others equate the up and down eigenvalues.

The evolution equation for the Cabibbo angle is given by [10]

$$\begin{aligned} \frac{d}{dt} \sin\theta_C = & -\frac{3}{2} \sin\theta_C \cos^2\theta_C \left\{ ({d_1}^2 + {d_2}^2) \left(\frac{{u_1}^2 - {u_2}^2}{{d_1}^2 - {d_2}^2}\right) \right. \\ & \left. + ({u_1}^2 + {u_2}^2) \left(\frac{{d_1}^2 - {d_2}^2}{{u_1}^2 - {u_2}^2}\right) \right\} , \end{aligned} \tag{4.3}$$

where the notation is as in Section 3. For reasonable values of the Yukawa couplings, the terms in parentheses tend to divide out, and the velocity of $\sin\theta_C$

is approximately proportional to the trace T_Q. For heavy quarks, T_Q is rather large, so the Cabibbo angle runs fairly quickly.

In Figures 12 and 13 we compare the running of the Cabibbo angle to that of the trace T_Q. In Figure 12 we see that the radial fixed point is reached for most initial conditions. We also see that $\sin\theta_C$ is strongly renormalized. As long as there is not a misidentification of families at the grand unification scale (corresponding to $\sin\theta_C > 1/\sqrt{2}$), the low energy Cabbibo angles renormalize by at least a factor of two. Note that the heavier the quarks, the greater is the renormalization of $\sin\theta_C$. The variations of $\sin\theta_C$ and T_Q with energy are shown in Figure 13. Again we see that for heavy quarks, the Cabibbo angle renormalizes quickly, but not as fast as the trace T_Q.

Equation (4.3) also applies to the Cabibbo mixing between one heavy quark and one light quark. If $u_1 \gg u_2$ and $d_1 \gg d_2$, equation (4.3) reduces to the following form,

$$\frac{d}{dt}\sin\theta_C \;=\; -\,\frac{3}{2}\sin\theta_C\cos^2\theta_C\,T_Q\;. \tag{4.4}$$

This shows explicitly that the mixings between heavy and light quarks tend to vanish just as quickly as the mixings between the light quarks themselves.

Equation (4.1) does not necessarily imply that Cabibbo angles *vanish* at the quark fixed point. They can also approach $\pi/2$. This can be seen from equation (4.3). If the lightest up-type quark is not predominantly the weak partner of the lightest down-type quark, then $(u_1 - u_2)(d_1 - d_2) < 0$, and θ_C increases with time. This is also clear in Figure 14, where we have plotted $\sin\theta_C$ against $(u_1 - u_2)(d_1 - d_2)$. Depending on the sign of the product, the Cabibbo angle runs either to zero or $\pi/2$. We see that the weak multiplet structure at the grand unification scale does not determine weak multiplet structure at the fixed point. With two heavy families, the multiplet structure at the fixed point is governed entirely by the mass spectrum at M_X. Up- and down-type quarks closest in mass run together to form properly paired weak doublets.

Whether the Cabibbo angles approach 0 or $\pi/2$ is essentially a matter of convention. In what follows it is most convenient to define θ_C to run to 0. In this case, there are many fixed points, corresponding to all possible pairings of the mass eigenvalues. With two heavy families, there are two fixed points, one with $\theta_C = 0$, $u_1 = d_1$, $u_2 = d_2$, and the other with $\theta_C = 0$, $u_1 = d_2$, $u_2 = d_1$. The first corresponds to properly paired weak doublets, and the second to maximal mixing. We have seen that the first fixed point is stable, and that the second is not. A similar analysis can be carried out in the general case of N_F total families. Barring degeneracies, there are $N_F!$ fixed points, related to each other by permutations. Expanding the Kobayashi-Maskawa matrix around unity, $V_L = 1 + \Theta$, it is easy to show that

$$\begin{aligned} \frac{d\Theta_{ij}}{dt} &= -\frac{3}{2}\Theta_{ij}\left\{(d_i{}^2 + d_j{}^2)\left(\frac{u_i{}^2 - u_j{}^2}{d_i{}^2 - d_j{}^2}\right)\right. \\ &\left. + (u_i{}^2 + u_j{}^2)\left(\frac{d_i{}^2 - d_j{}^2}{u_i{}^2 - u_j{}^2}\right)\right\}, \end{aligned} \tag{4.5}$$

This equation implies that the only stable fixed point is the one with properly paired weak doublets. All the other fixed points are unstable.

Our final topic will be that of isospin breaking in the case of two heavy families. The evolution of u_i/d_j is as follows [10],

$$\begin{aligned} \frac{d}{dt}\log\left(\frac{u_i}{d_j}\right) &= -\frac{3}{2}\left\{(u_i{}^2 - d_j{}^2) + \cos^2\theta_C\,(u_j{}^2 - d_i{}^2)\right. \\ &\left. + \sin^2\theta_C\,(u_{j'}{}^2 - d_{i'}{}^2)\right\} + \frac{3}{5}g_1^2, \end{aligned} \tag{4.6}$$

where $i' \neq i$ and $j' \neq j$. In Figure 15 we plot u_1/d_1 for a variety of initial conditions. As before, we see that the isospin breaking renormalizes subtantially between the grand unification scale M_X and the weak scale M_W.

5. Fixed Points and Initial Conditions

In this section we illustrate the role played by the initial conditions in determining the low energy spectrum of a grand unified theory with N_H heavy families. We assume that the theory has N_H heavy quark doublets, no Cabibbo mixings, and we neglect all lepton masses. This system is completely characterized by $2N_H$ diagonal Yukawa couplings u_i and d_i, where $i = 1, \ldots, N_H$. (The vanishing of the Cabibbo angles at all energies is guaranteed by family conservation.) In this case, the evolution equations (2.1) reduce to

$$\begin{aligned} \frac{d}{dt} u_i &= u_i \left\{ G_U - T - \frac{3}{2}({u_i}^2 - {d_i}^2) \right\} \\ \frac{d}{dt} d_i &= d_i \left\{ G_D - T - \frac{3}{2}({d_i}^2 - {u_i}^2) \right\} . \end{aligned} \tag{5.1}$$

where T and G_Y are given in (2.2). In the usual approximation $G_U = G_D = G_Q$, equations (5.1) imply

$$\frac{d}{dt} \log \frac{u_i}{d_i} = -3({u_i}^2 - {d_i}^2) . \tag{5.2}$$

The radial fixed point condition (2.4) is given by

$$3 \sum_{i=1}^{N_H} ({u_i}^2 + {d_i}^2) = \overline{G}_Q , \tag{5.3}$$

while the angular fixed point condition (2.5) is simply

$$u_i = d_i . \tag{5.4}$$

Equation (5.2) admits $N_H - 1$ conservation laws,

$$\frac{d}{dt} \log \frac{u_i d_i}{u_j d_j} = 0 , \tag{5.5}$$

where no sum on i or j is implied.

At the fixed point (5.3) and (5.4), the $2\,N_H$ low energy Yukawa couplings are determined by the $N_H + 1$ fixed point conditions,

$$\begin{aligned} u_i &= d_i \equiv q_i \ , \\ 6 \sum_{i=1}^{N_H} {q_i}^2 &= \overline{G}_Q \ , \end{aligned} \tag{5.6}$$

together with $N_H - 1$ initial conditions

$$\frac{q_i}{q_j} = \sqrt{\frac{{u_i}^0 {d_i}^0}{{u_j}^0 {d_j}^0}} \ . \tag{5.7}$$

Here ${u_i}^0$ and ${d_i}^0$ are the $2\,N_H$ initial Yukawa couplings at the scale M_X. Combining (5.6) and (5.7), one can solve for the low energy spectrum in terms of the initial conditions ${u_i}^0$ and ${d_i}^0$, as well as the effective gauge coupling $\overline{G}_Q$:

$${u_i}^2 = {d_i}^2 = \frac{1}{6} \left(\frac{{u_i}^0 {d_i}^0}{\sum_j {u_j}^0 {d_j}^0} \right) \overline{G}_Q \ . \tag{5.8}$$

Equation (5.8) gives the full low energy spectrum of a grand unified theory with N_H heavy quarks and no Cabibbo mixings. It is valid to the accuracy to which the fixed point is reached.

6. Light Fermions in the Presence of Heavy Families

For our final topic we study the renormalization of light fermions in the presence of N_H heavy families. We assume that there are no Cabibbo mixings between the light and heavy generations. This assumption is physically reasonable in light of the results of Section 4.

Let u and d denote the *matrices* of the Yukawa couplings of the light up- and down-type quarks. They obey the following evolution equations,

$$\begin{aligned} \frac{d}{dt} u &= u[G_U - T] \\ \frac{d}{dt} d &= d[G_D - T] , \end{aligned} \tag{6.1}$$

where T is defined in (2.2). In equation (6.1) we have neglected the light fermion contributions S_u and S_d since they are much smaller than G_Y and T. To a very good approximation, T is just a trace over the heavy families. It does not depend on the light Yukawas. In this case, $[\dot{u}, u] = 0$ and $[\dot{d}, d] = 0$, and it is easy to solve for u and d,

$$\begin{aligned} u(t) &= u(0) \exp \int_0^t dt' \, (G_U - T) \\ d(t) &= d(0) \exp \int_0^t dt' \, (G_D - T) . \end{aligned} \tag{6.2}$$

In a similar way, we find

$$e(t) = e(0) \exp \int_0^t dt' \, (G_E - T) . \tag{6.3}$$

The exponentials in (6.2) and (6.3) are simply numbers, while u, d and e are matrices. This implies that the Cabibbo mixings between light fermions and the mass ratios u_i/u_j, d_i/d_j do not get renormalized. The Cabibbo mixings and the mass ratios retain their initial values all the way down to the weak scale M_W.

Equation (6.2) also implies that the u_i/d_j remain (essentially) constant. Their

renormalization is given by

$$\frac{u_i}{d_j} = \frac{u_i(0)}{d_j(0)} \exp \int_0^{t_W} dt' \, (G_U - G_D) \, . \tag{6.4}$$

Since $G_U \simeq G_D$, the ratios barely run. In contrast, the light quark-to-lepton mass ratios renormalize significantly. Their evolution equations take the following form,

$$\begin{aligned} \frac{u_i}{e_j} &= \frac{u_i(0)}{e_j(0)} \exp \int_0^{t_W} dt' \, (G_U - G_E) \\ \frac{d_i}{e_j} &= \frac{d_i(0)}{e_j(0)} \exp \int_0^{t_W} dt' \, (G_D - G_E) \, . \end{aligned} \tag{6.5}$$

Note that all the ratios renormalize by the same amount. This renormalization does *not* depend on the spectrum of heavy families; it only depends of the *total* number of families through the gauge couplings G_Y. Theories with more heavy families give larger u_i/e_j and d_i/e_j renormalizations. In the case of four families, we find that the quark-to-electron mass ratios renormalize by a factor of 2.3 (between t_X and t_W). With eight families, we find that the factor increases to about nine.

It is interesting to compare the evolution of light fermions in the presence and absence of heavy families. When heavy families are present, the evolution of the light quarks is controlled by their heavy partners. The light quarks first track the heavies, and then all quarks stop running when the radial fixed point is reached. The leptons, however, never stop running. Their masses decrease continuously with energy. This behavior is illustrated in Figure 16(a) for the case of one heavy family. Note that the light-to-heavy quark mass ratio remains constant with time, and that the lepton evolves continuously. If there are no heavy families, the story is very different. The leptons evolve slowly because of their small SU(2) $\times$ U(1)

couplings. The quarks, however, renormalize significantly because of their strong SU(3) color interactions [11]. The evolution of a typical pair of light quark and lepton Yukawas is shown in Figure 16(b). As expected, the lepton stays constant, while the quark increases by about a factor of three. Note, however, that the quark-to-lepton mass ratios renormalize identically in the two figures. They depend only on the number heavy families through the gauge couplings G_Y.

7. Conclusions

In this paper we have studied the renormalization of heavy quark and lepton masses. We have made two fundamental assumptions. The first is that of a SU(3) $\times$ SU(2) $\times$ U(1) desert extending from the weak scale M_W to the grand unification scale M_X. The second is that of perturbative unification. We assume that perturbation theory is valid between M_W and M_X. This means that all gauge and Yukawa couplings must be $\lesssim 10$ throughout the entire SU(3) $\times$ SU(2) $\times$ U(1) desert.

We have shown that the above assumptions lead to strict bounds on the quark and lepton masses,

$$\begin{aligned} \sum {M_Q}^2 &\lesssim (355 \text{ GeV})^2 \\ \sum {M_L}^2 &\lesssim (330 \text{ GeV})^2 \, . \end{aligned} \tag{7.1}$$

These bounds imply that theories with N_H heavy families must have at least one quark *and* one lepton of mass less than $250/\sqrt{N_H}$ GeV. We have also demonstrated that the mixing angles among heavy families (as well as between heavy and light families) tend to be small. This implies that some heavy quarks should have relatively long lifetimes. Finally, we have also shown that isospin breaking tends to be small in the heavy quark sector.

REFERENCES

1. M. Chanowitz, M. Furman and I. Hinchliffe, Phys. Lett. 78B (1978) 285.
2. M. Veltman, Nucl. Phys. B123 (1979) 89.
3. P. Hung, Phys. Rev. Lett. 42 (1979) 873; H. D. Politzer and S. Wolfram, Phys. Lett. 82B (1979) 242; (E) 83B (1979) 421.
4. B. Pendleton and G. Ross, Phys. Lett 98B (1981) 291.
5. C. Hill, Phys. Rev. D24 (1981) 691.
6. E. Paschos, Santa Barbara preprint NSF-ITP-84-69 (1984).
7. T. Cheng, E. Eichten and L. Li, Phys. Rev. D9 (1974) 2259; M. Machacek and M. Vaughn, Nucl. Phys. B236 (1984) 221.
8. N. Cabibbo, L. Maiani, G. Parisi and R. Petronzio, Nucl. Phys. B158 (1979) 295.
9. H. B. Nielsen and M. Ninomiya, Nucl. Phys. B141 (1979) 153; J. Iliopoulos, D. Nanopoulos and T. Tomaras, Phys. Lett. 94B (1980) 141; I. Antoniadis, J. Iliopoulos and T. Tomaras, Nucl. Phys. B227 (1983) 447.
10. E. Ma and S. Pakvasa, Phys. Rev. D20 (1979) 2899.
11. M. Chanowitz, J. Ellis and M. Gaillard, Nucl. Phys. B128 (1977) 506; A. Buras, J. Ellis, M. Gaillard and D. Nanopoulos, Nucl. Phys. B135 (1978) 66.

FIGURE CAPTIONS

1. The evolution of T_Q and T_L with t, for $N_F = 8$ families and various initial conditions. The arrows indicate the flow of increasing t. The dotted lines denote the radial quark and lepton fixed points.

2. (a) The trace T_Q at M_W as a function of the trace T_Q at M_X, for $N_F = 8$ and $T_L = 0$. The dotted line denotes the radial quark fixed point. For $T_Q(M_X) > 0.1$, the fixed point is reached in physical time.
   (b) $T_L(M_W)$ as a function of $T_L(M_X)$, for $N_F = 8$ and $T_Q = 0$.

3. The QCD coupling $\alpha_{\rm QCD}$ as a function of energy for $N_F = 4$, 8 and 9. For $N_F = 9$, $\alpha_{\rm QCD}$ blows up at 10^{10} GeV.

4. The evolution of the Yukawa couplings u and d with energy for one heavy family and $N_F = 4$. The radial quark fixed point is denoted by the dotted line. Trajectory (α) shows the evolution when one quark is heavy and the other very light. Trajectory (β) gives the evolution when both quarks are light. Neither (α) nor (β) reach the fixed point in physical time.

5. The evolution of $T_Q = u^2 + d^2$ with energy for the initial conditions of Figure 4. The dotted line corresponds to the quark fixed point.

6. Typical evolution of T and G_Q for $N_F = 4$. The arrow indicates the weak scale M_W. At energies far below M_W, the trace T tracks the gauge couplings G_Q (see Ref. 4).

7. The evolution of the Yukawa coupling of the charged lepton in a single heavy family. We have set $N_F = 4$ and all neutrino masses to zero. Note that below 10^{13} GeV, e evolves with a constant logarithmic velocity.

8. The evolution of the quark Yukawa couplings for two heavy families with $N_F = 5$ and no Cabibbo mixings. At $M = M_X$, we have set $u_1 = d_1$ and $u_2 = d_2$. The dotted line denotes the radial quark fixed point. Note that the evolution preserves the polar angle θ.

9. The evolution of $T_Q = \Sigma(u_i^2 + d_i^2)$ for the initial conditions of Figure 8. The dotted line indicates the radial fixed point.

10. The evolution of the isospin splitting u/d and of the trace $T_Q = u^2 + d^2$ for one heavy family and $N_F = 4$. We have set $d = 1$ at the scale M_X. The dotted lines indicate the radial and angular quark fixed points. Because of the choice of initial conditions, the radial fixed point is not quite reached in physical times.

11. (a) The evolution of u/d with energy for the initial conditions of Figure 10. The dotted line indicates the angular fixed point.
    (b) The trace T_Q for the initial conditions of Figure 10.

12. The evolution of the Cabibbo angle and T_Q for two heavy families and $N_F = 5$. At the scale M_X we have taken $u_2 = d_2 = 2u_1 = 2d_1$. The radial fixed point is indicated by the dotted line. Trajectory (α) corresponds to the case of misidentified weak doublets. Trajectory (β) corresponds to a relatively small trace T_Q. We see that the radial fixed point is reached in physical time, but that the angular fixed point is not.

13. (a) The evolution of the Cabibbo angle with energy for the initial conditions of Figure 12. Trajectory (β) shows that a small trace induces a small renormalization of $\sin\theta_C$.
    (b) The trace T_Q for the initial conditions of Figure 12.

14. The Cabibbo angle $\sin\theta_C$ for $N_F = 5$, two heavy families, and $u_1 = d_1 = 2$, $d_2 = 1$ at the scale M_X. The evolution of $\sin\theta_C$ is such that the weak doublets at M_W are properly paired, independent of their initial conditions.

15. The isospin splitting u_1/d_1 as a function of energy for $N_F = 5$, $\sin\theta_C = 0$ and $u_2 = d_2 = 2$, $d_1 = 1$ at the scale M_X. The dotted line indicates the angular fixed point.

16. (a) The evolution of quarks and leptons as a function of energy for $N_F = 4$, with $u = d$ at the scale M_X. The solid lines denote the evolution of the

third and fourth families, and the dot-dashed line indicates the evolution of a typical charged lepton. Note that the light quark Yukawa tracks that of the heavy quark and that the lepton renomrmalizes with a constant logarithmic velocity.

(b) The evolution of a typical quark and lepton with $N_F = 4$, $u = d$ and no heavy families. The lepton barely runs. The light quark-to-quark ratio renormalizes by the same amount as in (a).

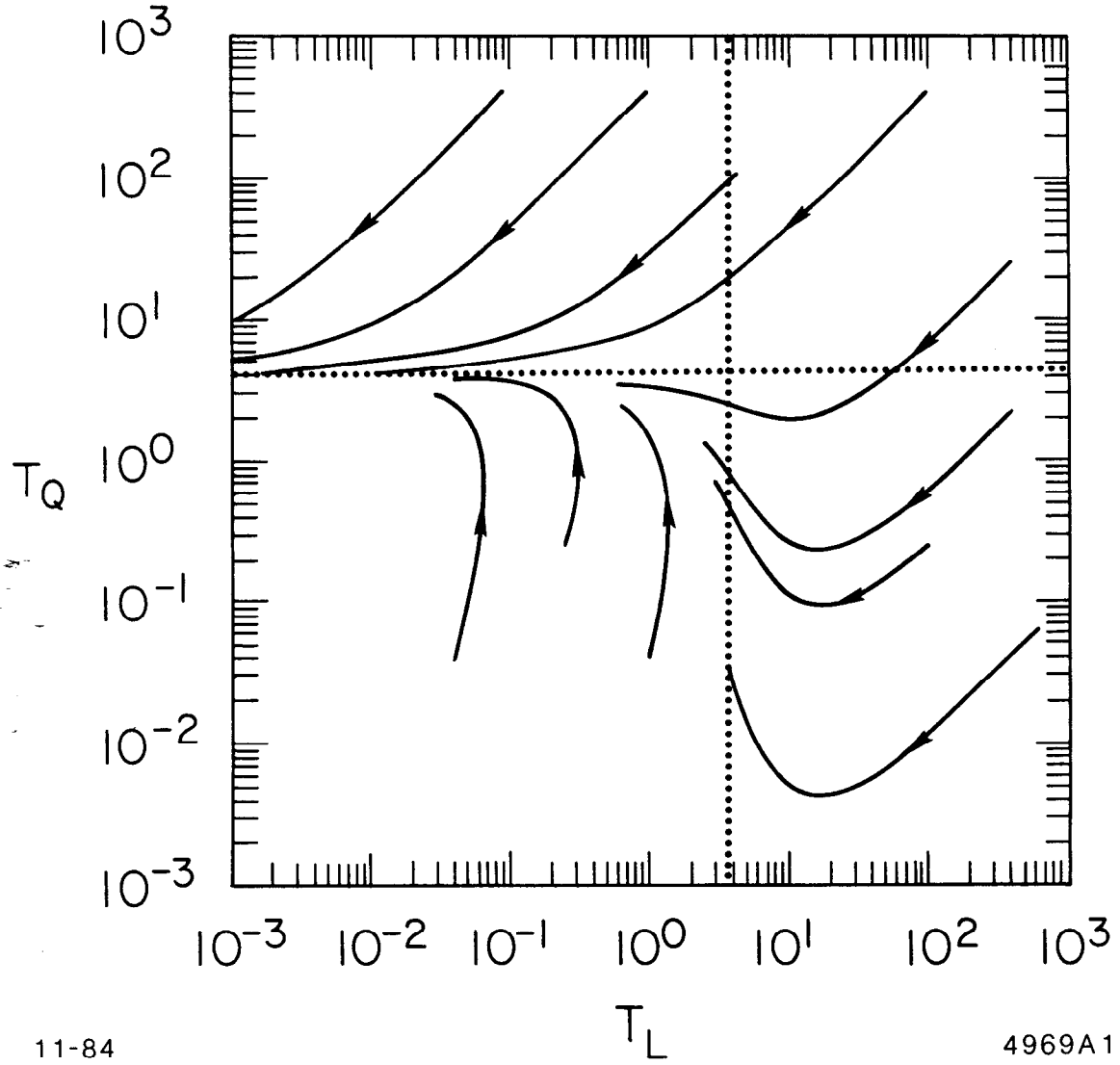
10^3
10^2
10^1
10^0
10^{-1}
10^{-2}
10^{-3}
T_Q
10^{-3} 10^{-2} 10^{-1} 10^0 10^1 10^2 10^3
T_L
11-84
4969A1

Fig. 1

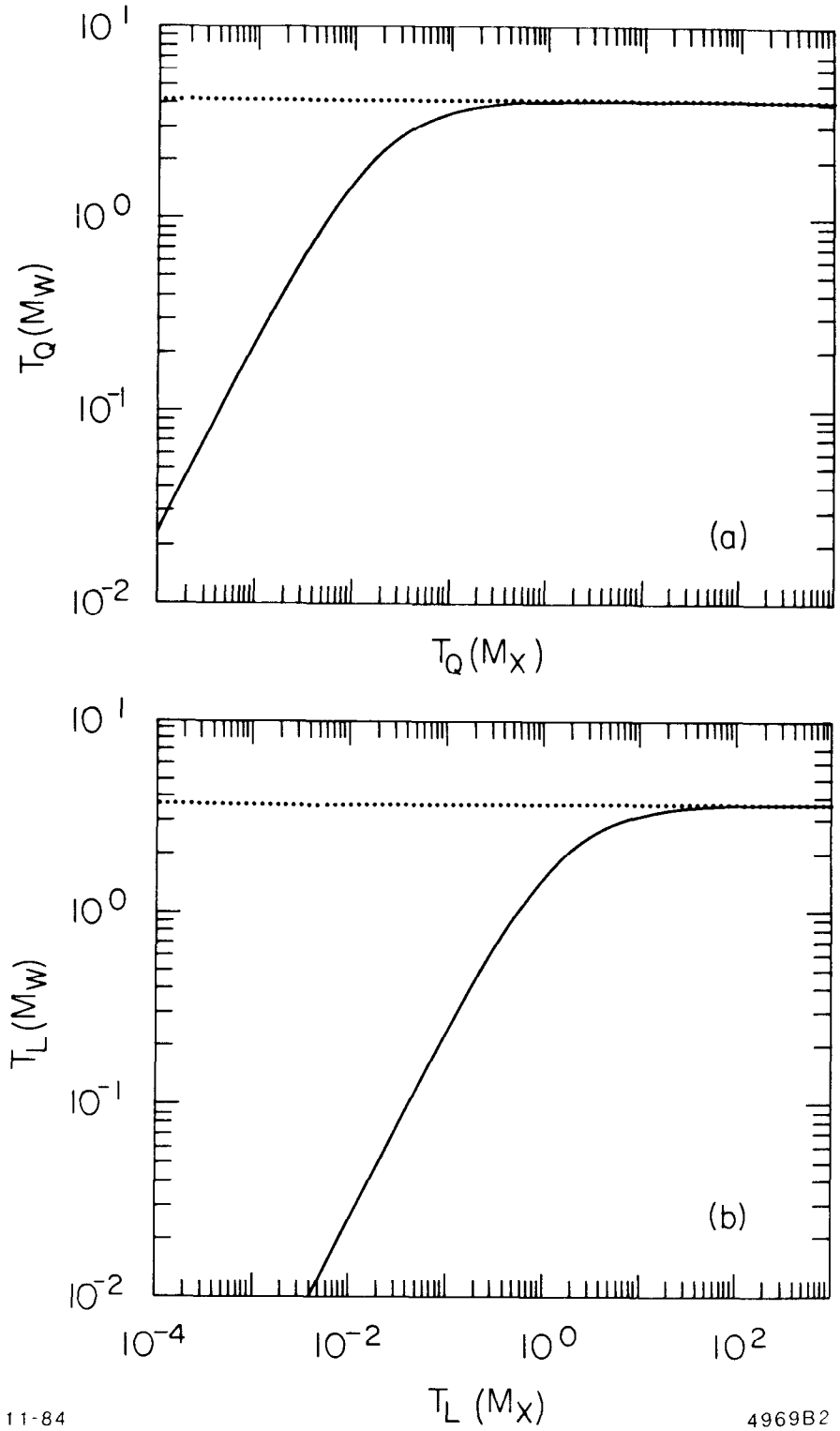
10^1
10^0
10^{-1}
10^{-2}
$T_Q(M_W)$
(a)
$T_Q(M_X)$
10^1
10^0
10^{-1}
10^{-2}
$T_L(M_W)$
(b)
10^{-4}
10^{-2}
10^0
10^2
$T_L(M_X)$
11-84
4969B2

Fig. 2

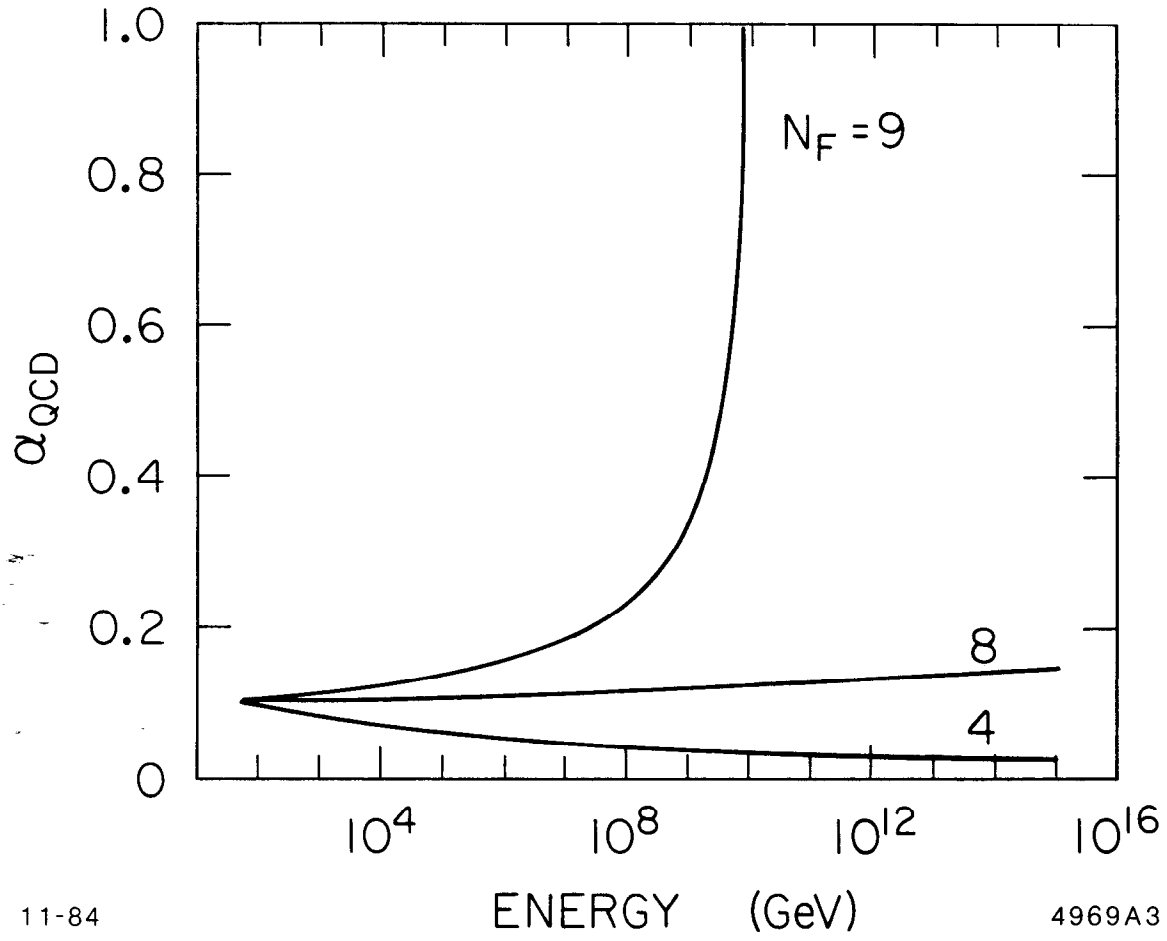
1.0
0.8
0.6
0.4
0.2
0
α_{QCD}
$N_F = 9$
8
4
10^4
10^8
10^{12}
10^{16}
ENERGY (GeV)
11-84
4969A3

Fig. 3

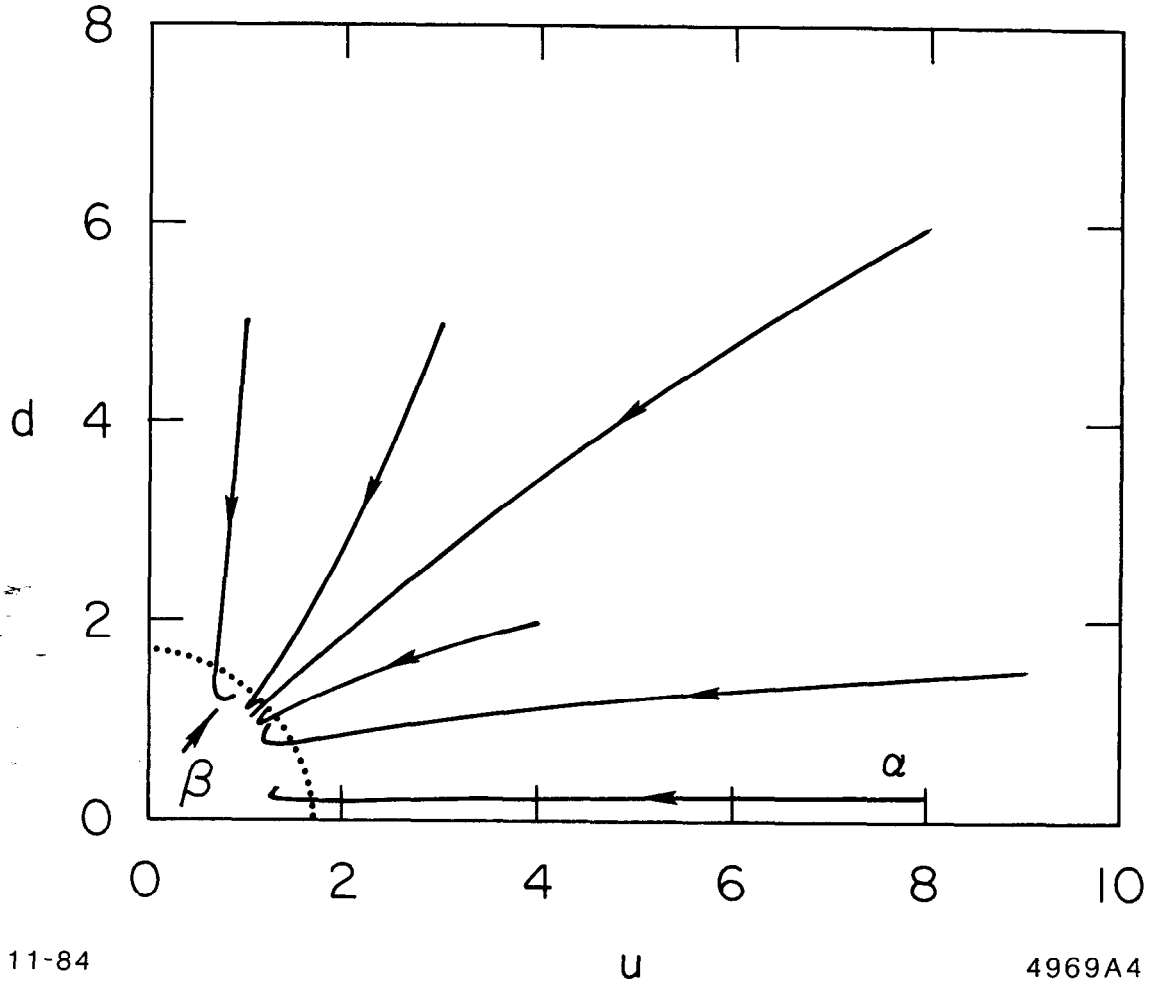

Fig. 4

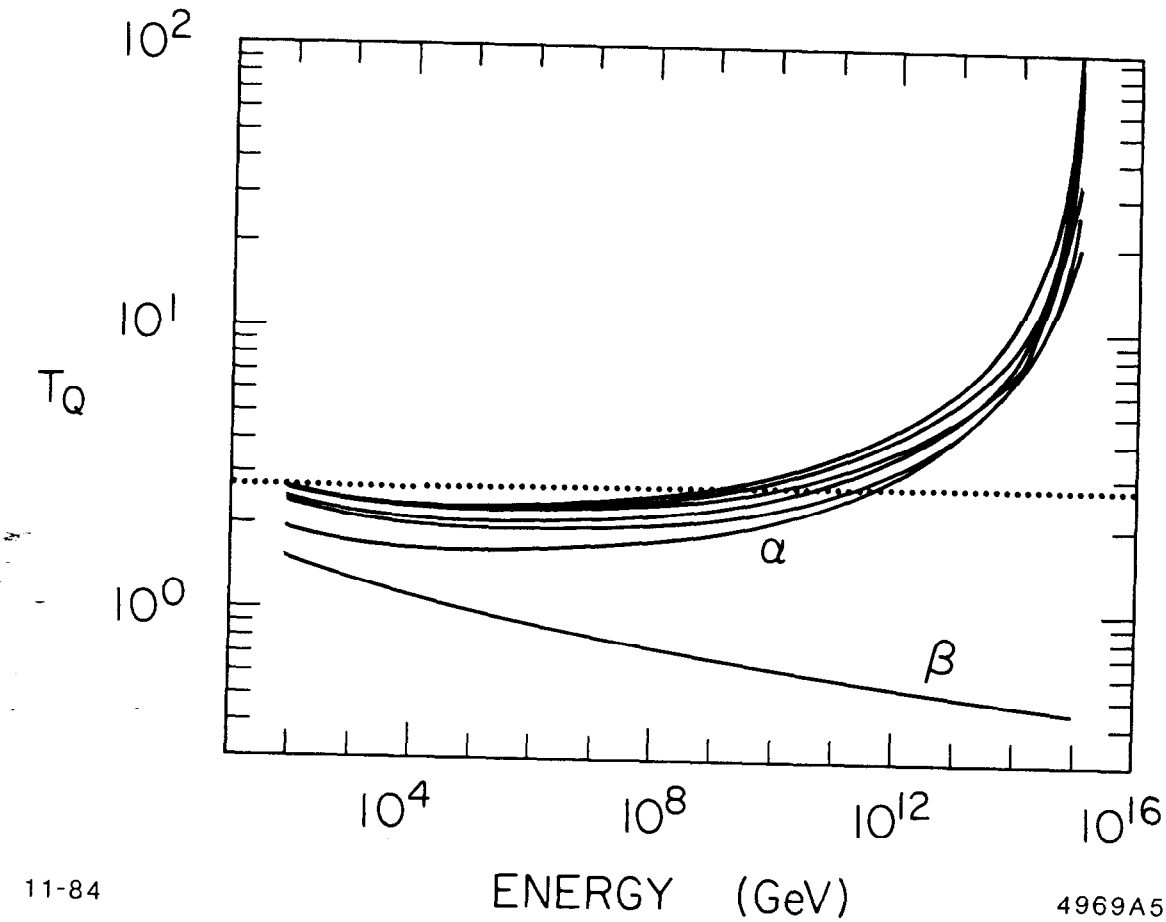
10^2
10^1
10^0
T_Q
α
β
10^4
10^8
10^{12}
10^{16}
ENERGY (GeV)
11-84
4969A5

Fig. 5

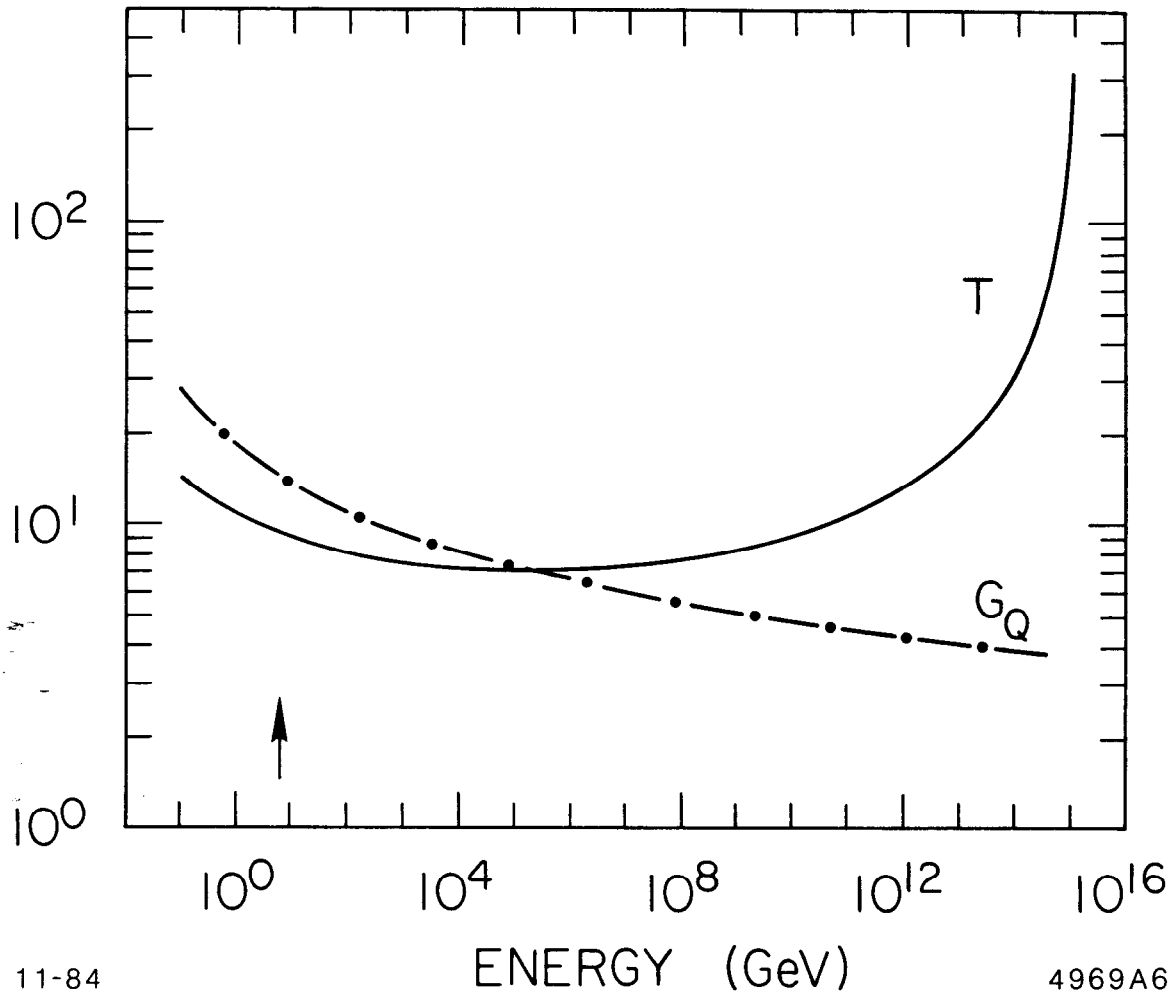

Fig. 6

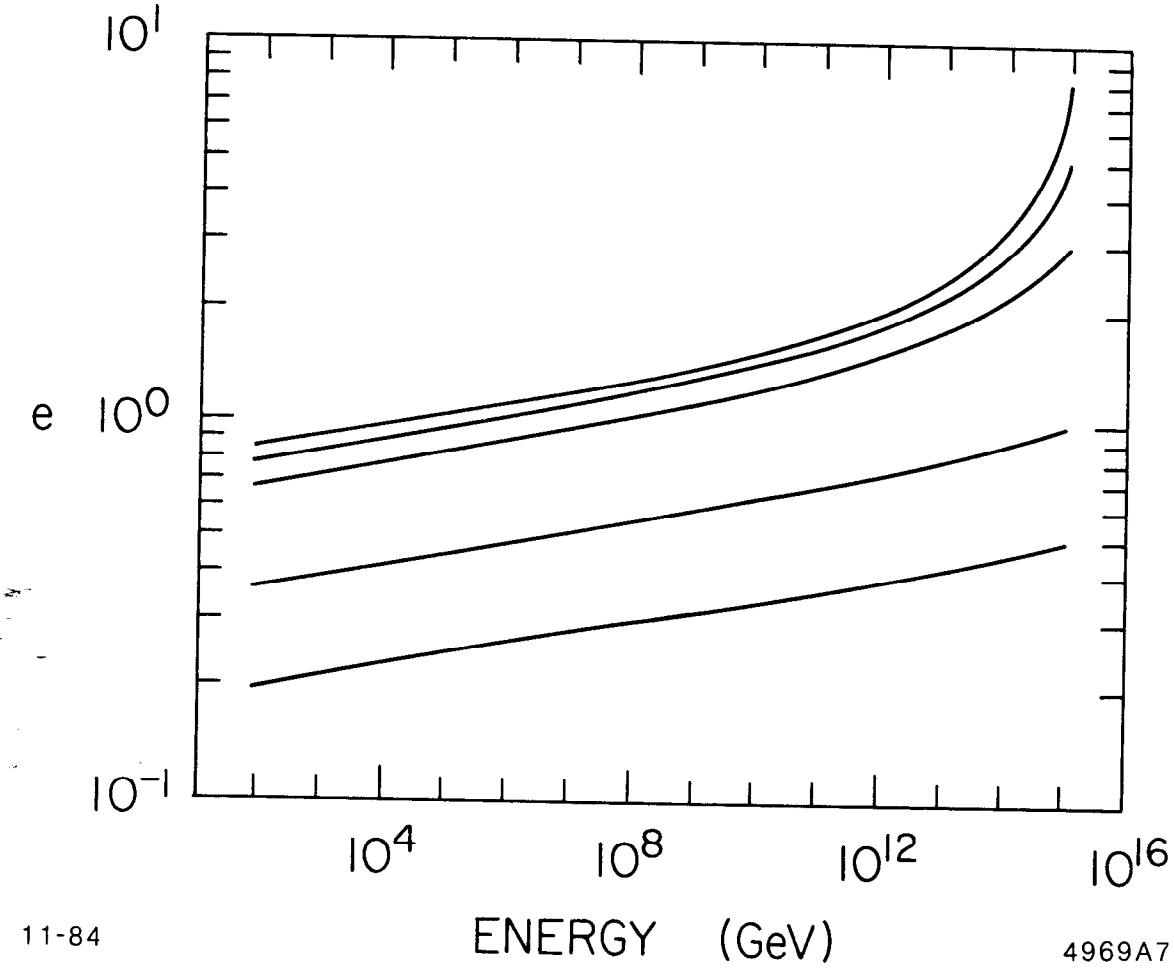

Fig 7

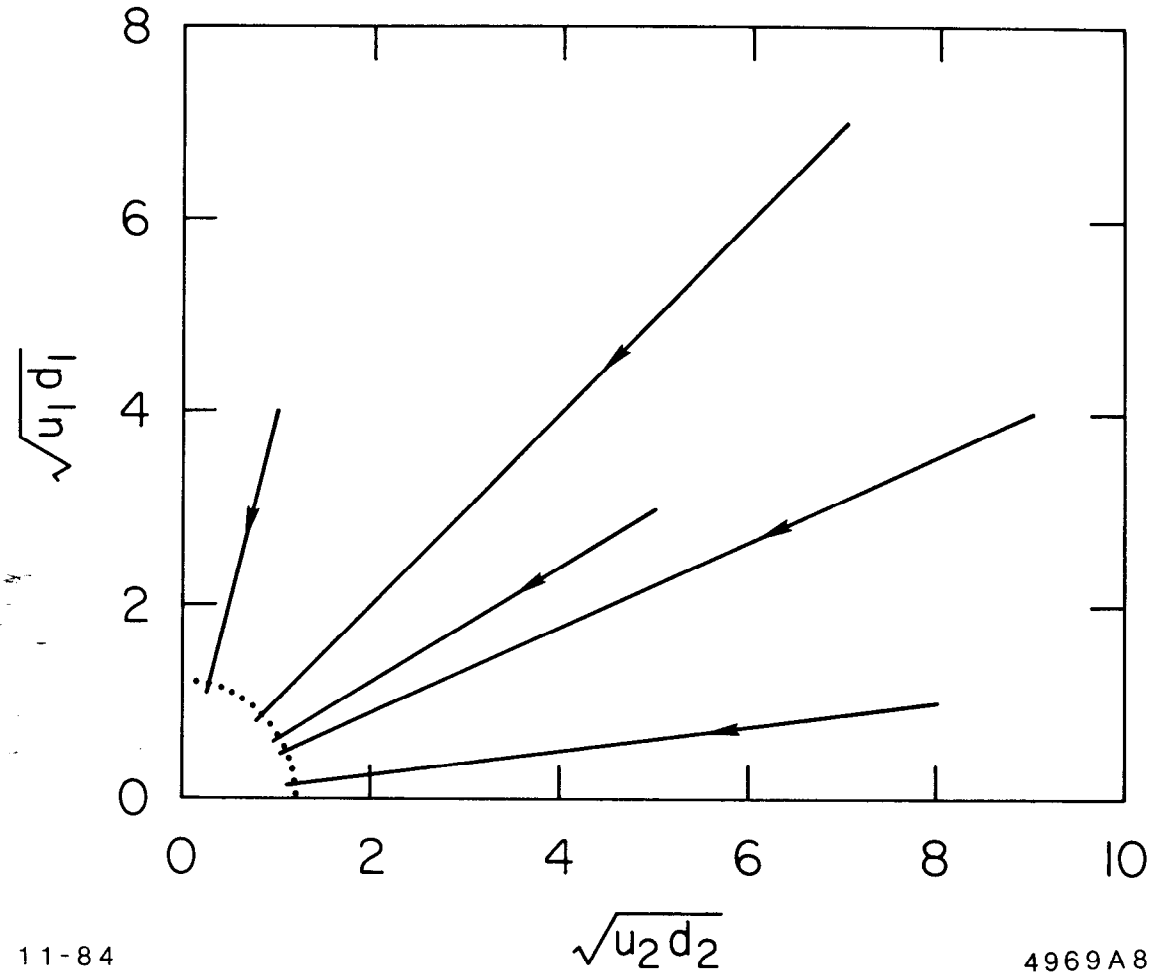

Fig. 8

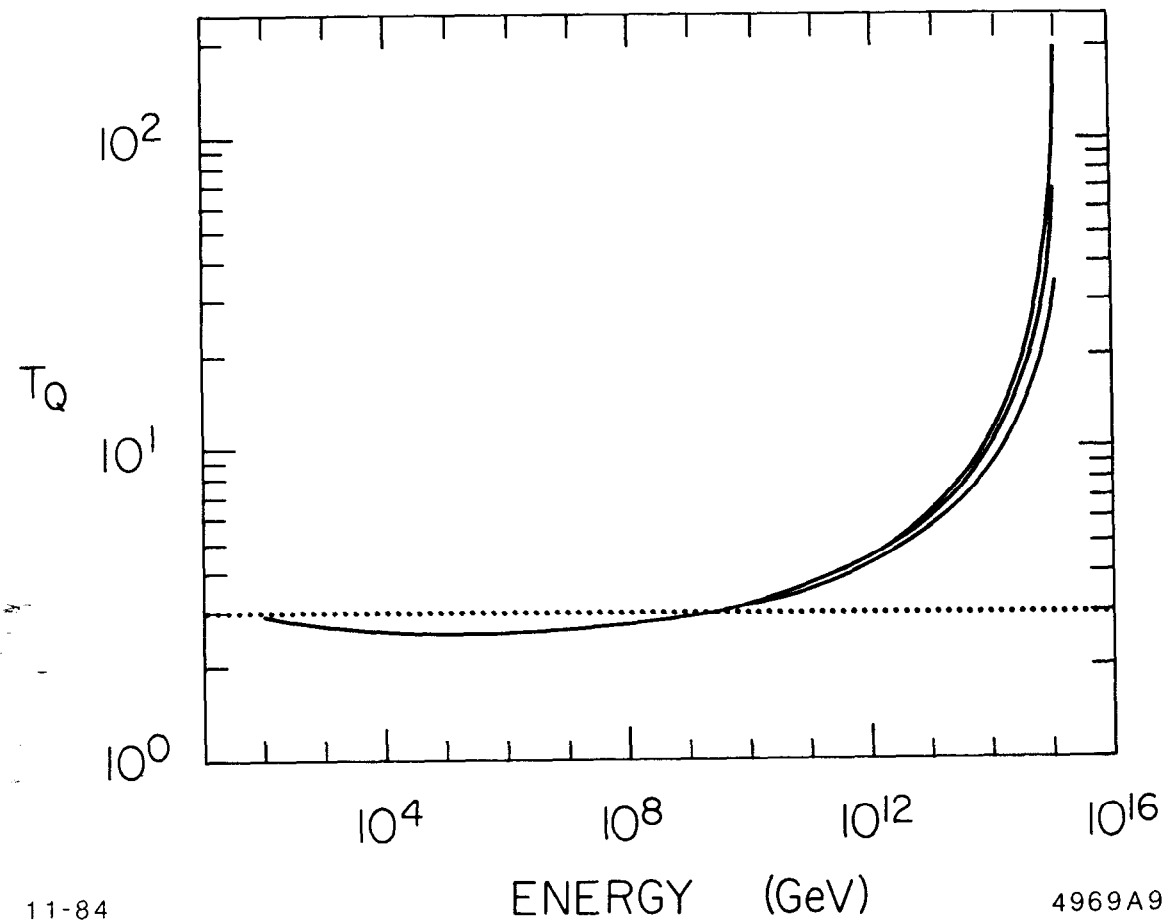

Fig. 9

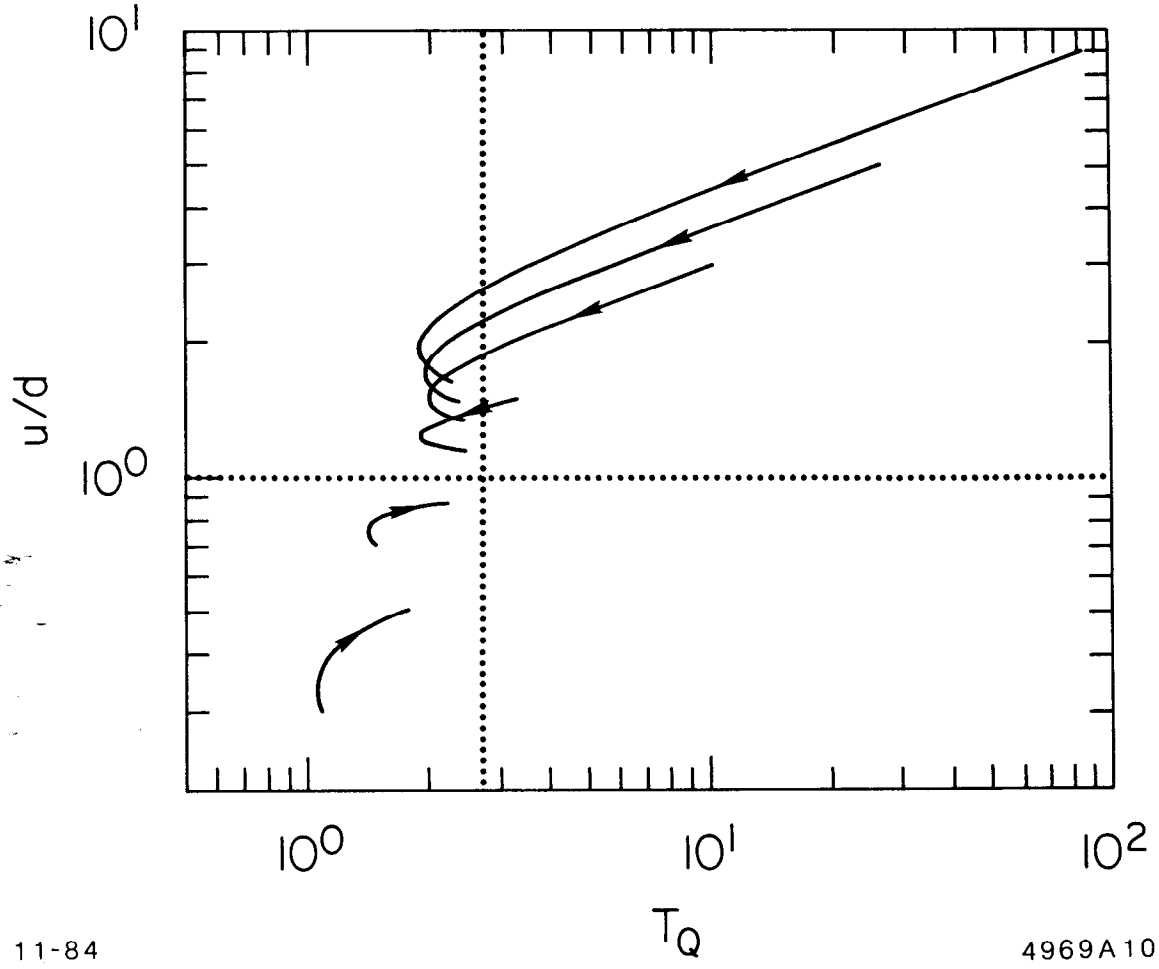

Fig. 10

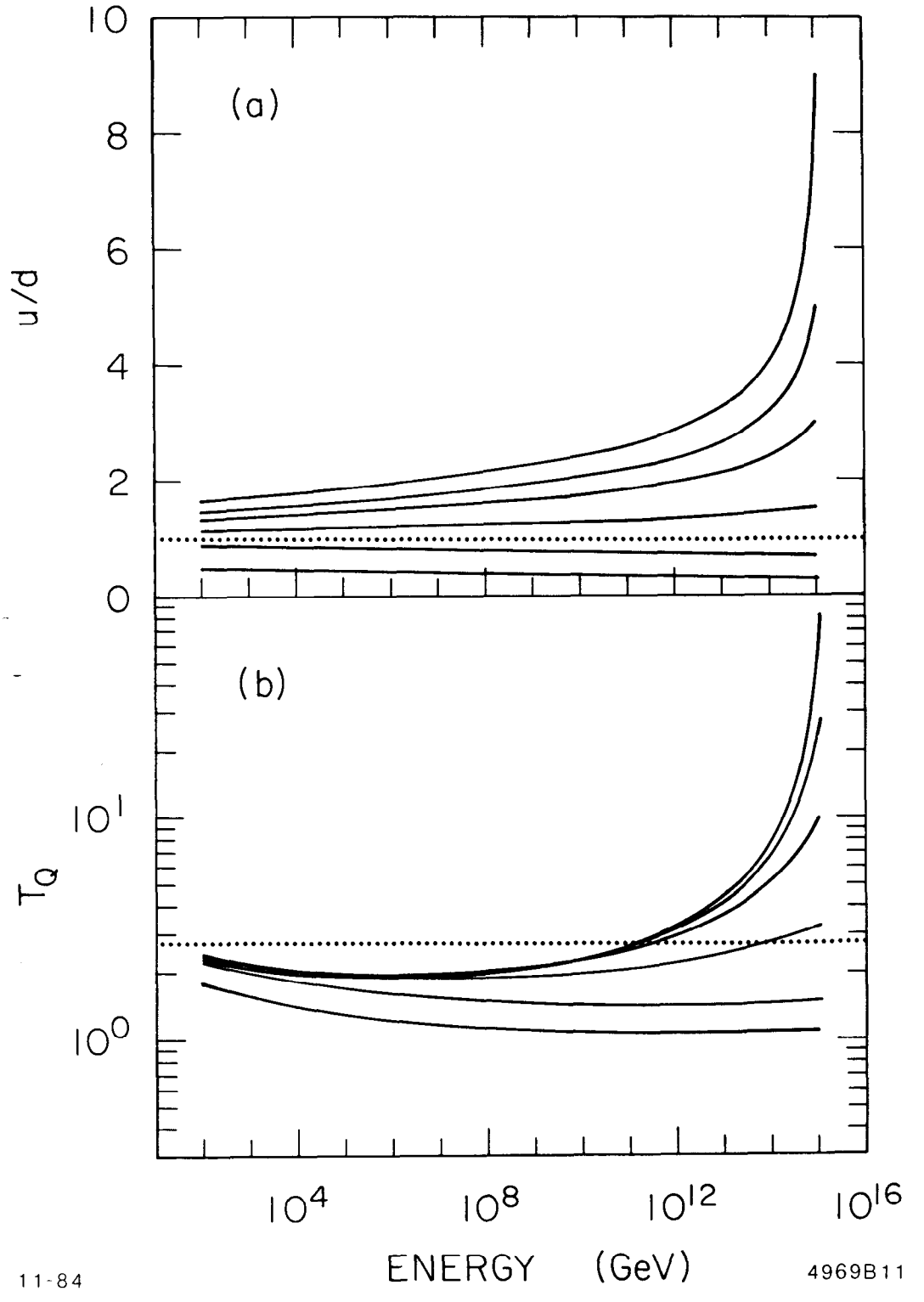
(a)
(b)
u/d
T_Q
10
8
6
4
2
0
10^1
10^0
10^4
10^8
10^{12}
10^{16}
ENERGY (GeV)
11-84
4969B11

Fig. 11

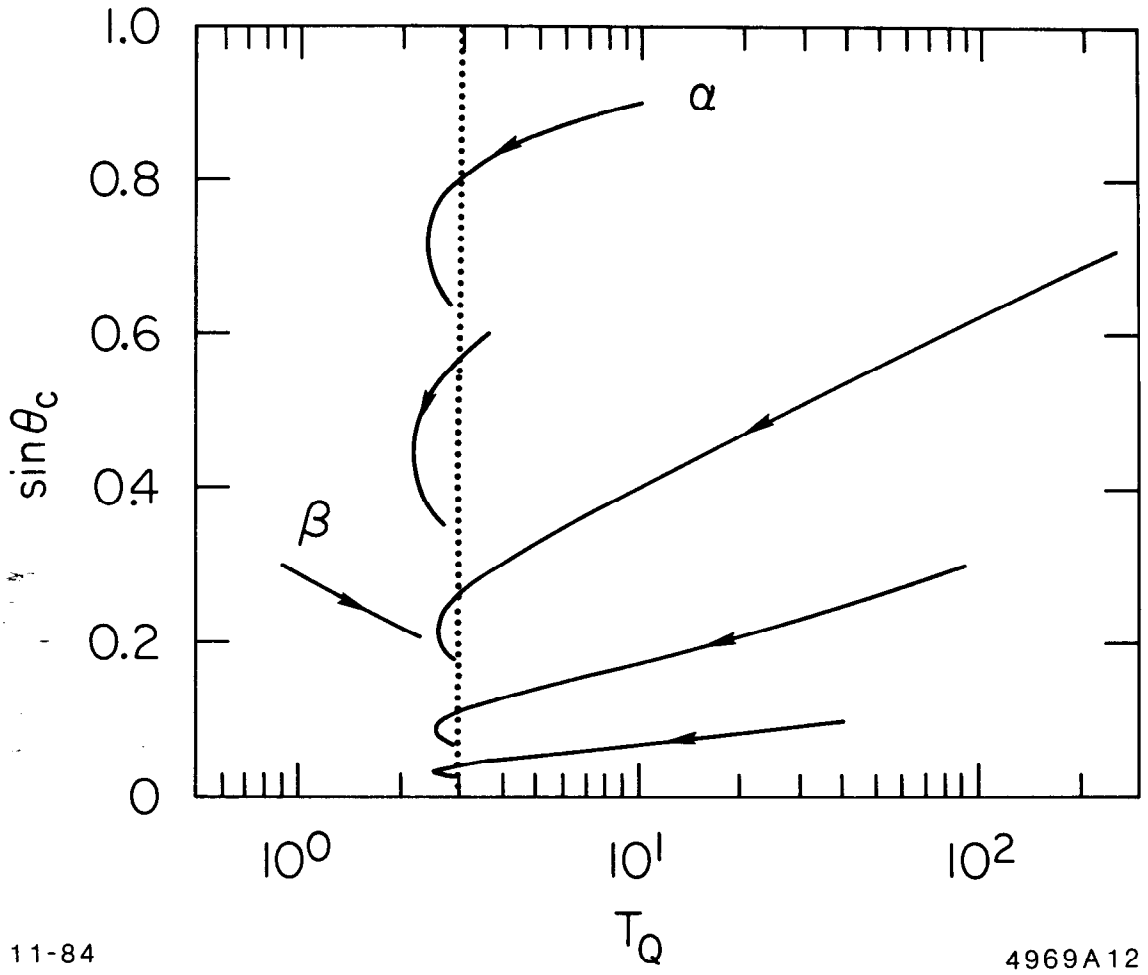

Fig. 12

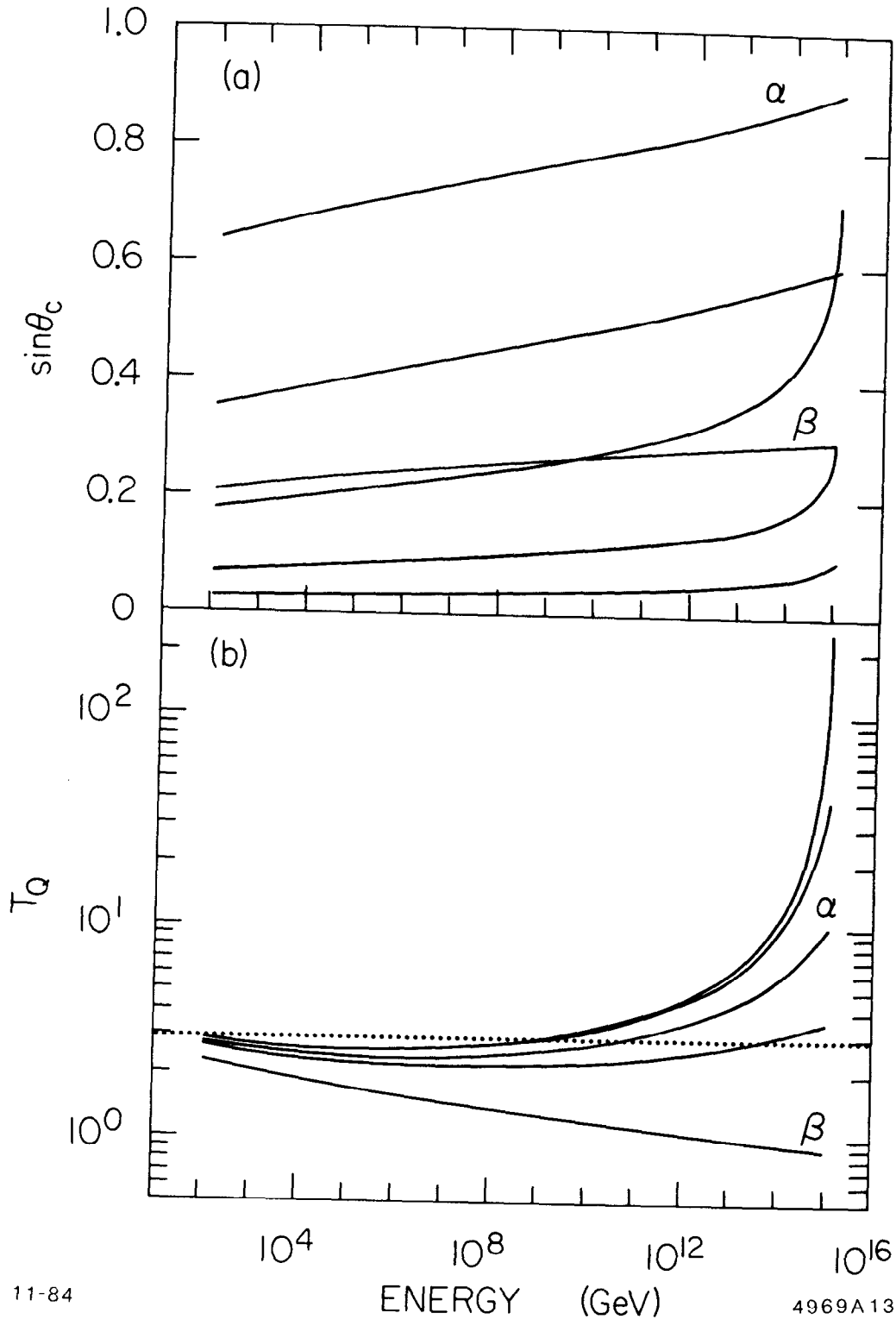
1.0
0.8
0.6
0.4
0.2
0
(a)
α
β
sinθc
(b)
10²
10¹
10⁰
α
β
TQ
10⁴
10⁸
10¹²
10¹⁶
ENERGY (GeV)
11-84
4969A13

Fig. 13

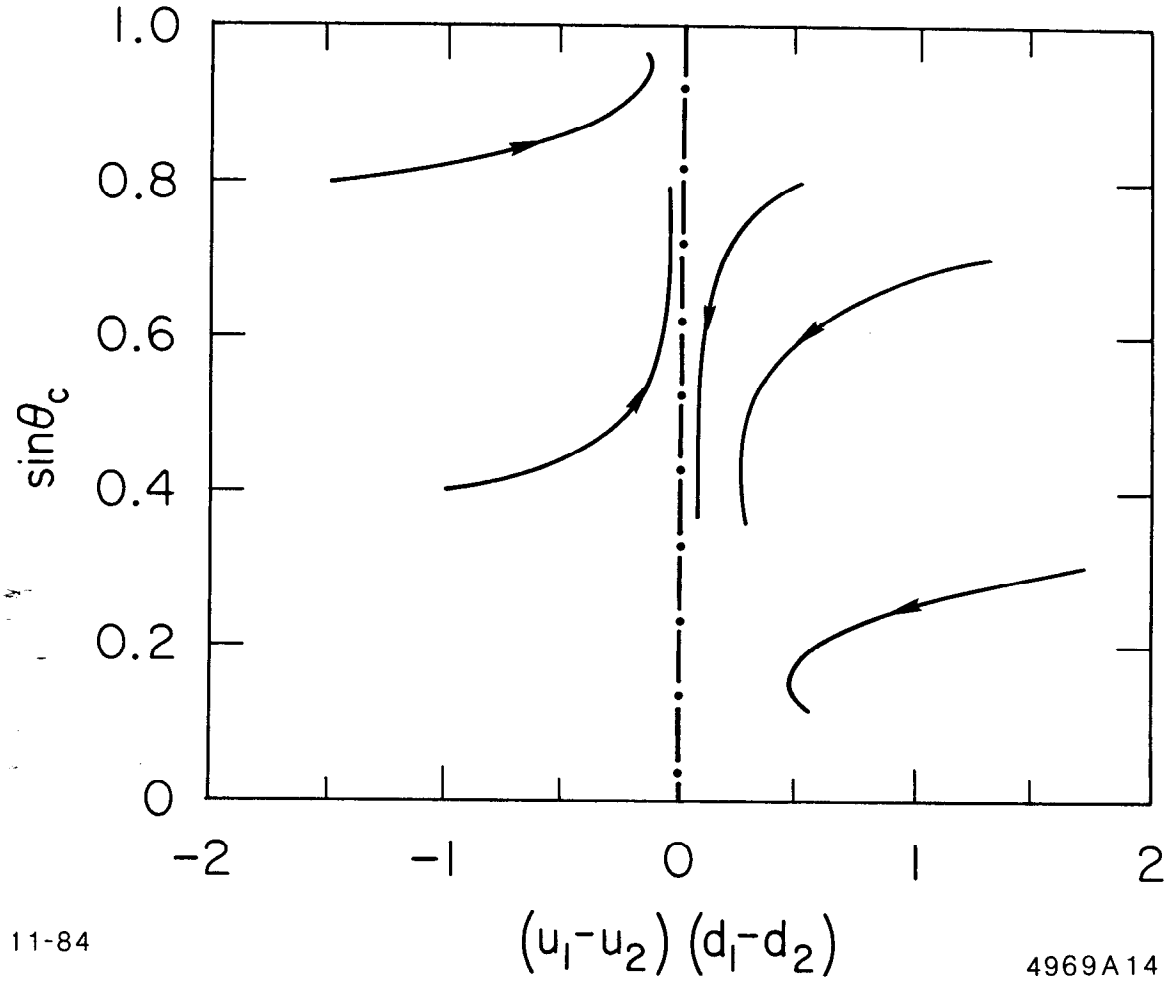

Fig. 14

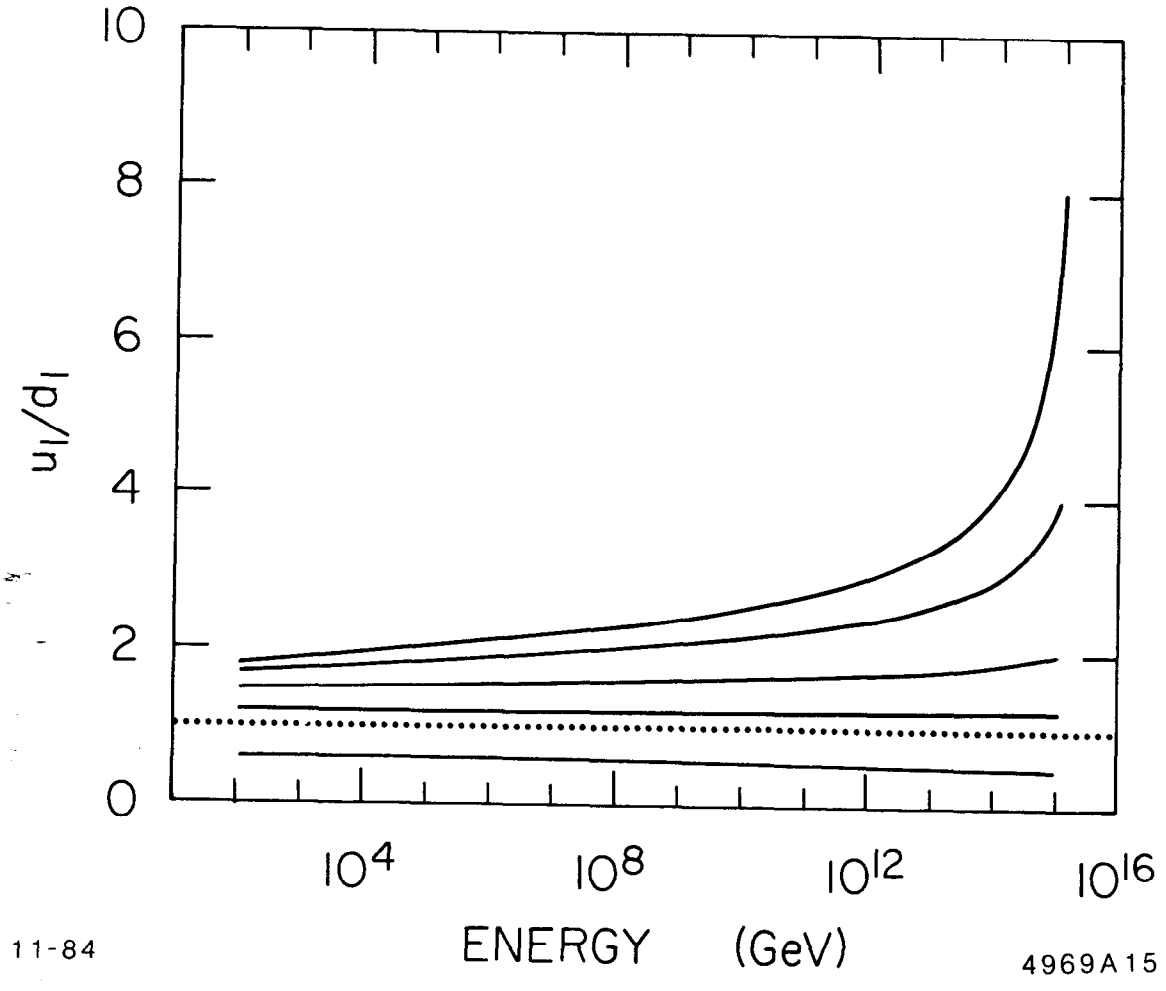

Fig. 15

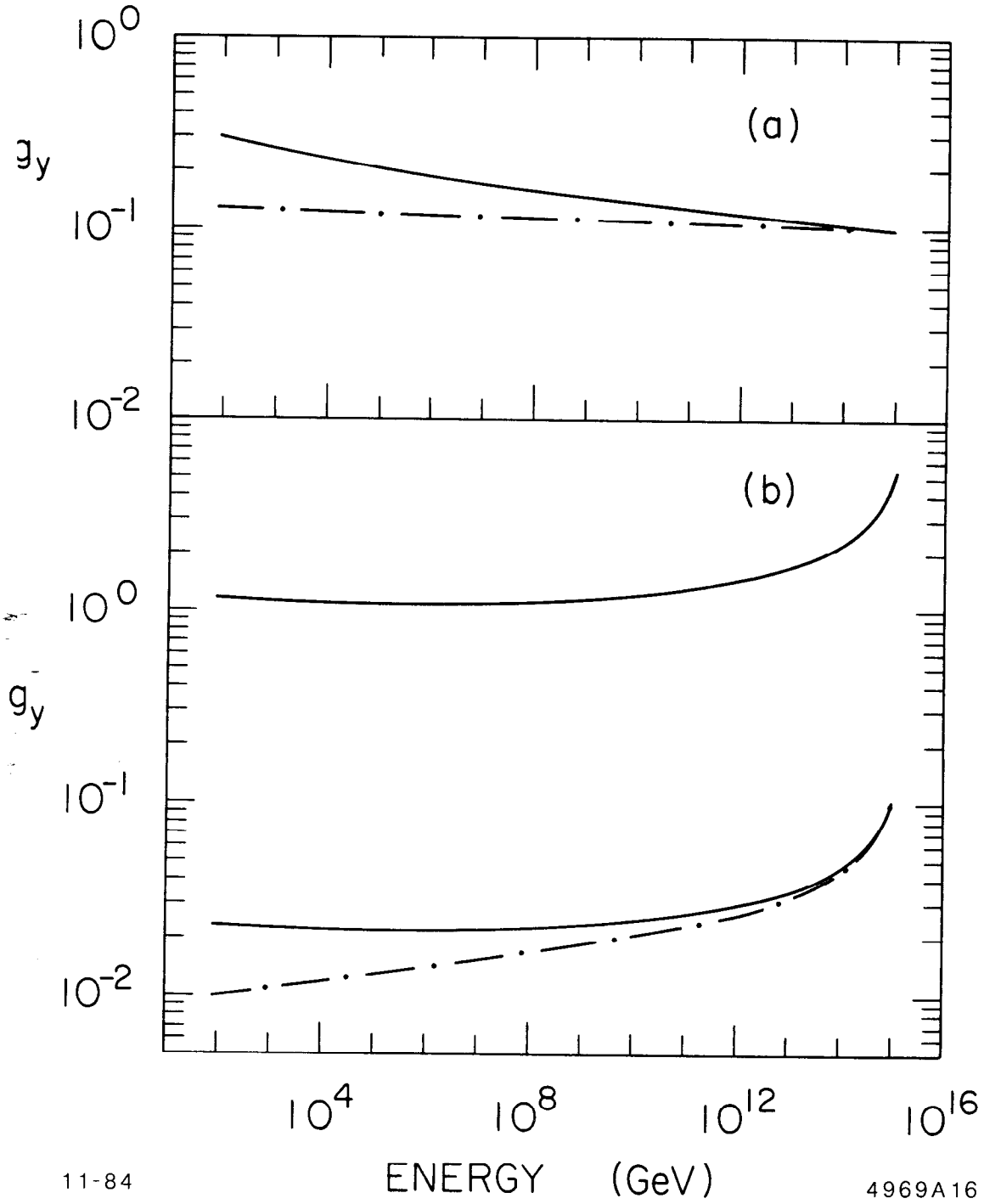
10^0
g_y
10^{-1}
10^{-2}
(a)
(b)
10^0
g_y
10^{-1}
10^{-2}
10^4
10^8
10^{12}
10^{16}
ENERGY (GeV)
11-84
4969A16

Fig. 16